Leadership in Sustainable Infrastructure

*Leadership en Infrastructures Durables*

Vancouver, Canada

May 31 – June 3, 2017/ *Mai 31 – Juin 3, 2017*

# NON-CONTACT NON-DESTRUCTIVE INFRARED THERMOGRAPHY BASED EVALUATION OF REINFORCED CONCRETE STRUCTURES

Rishi Gupta[1], Harsh Rathod[2,5], Balasubramanian Esakki [3], Sean Blaney[4]

[1] Assistant Professor, University of Victoria, Canada

[2] PhD Candidate, University of Victoria, Canada

[3] Associate Professor, Vel Tech University, India

[4] MASc. Candidate, University of Victoria, Canada

[5] hmrathod@uvic.ca

**Abstract:** Periodic inspection is an integral part of Structural Health Monitoring (SHM) for the safety and reliability of civil infrastructures. Conventional SHM procedures tend to be laborious, time consuming and capital intensive. Especially in the case of large span bridges, traditional methods are not effective for rapid full field monitoring. The proposed research work uses a non-contact non-destructive evaluation technique based on infrared thermography to detect the artificial defects in reinforced concrete slabs. For this work, a total of nine 1800 mm × 460 mm reinforced concrete slabs with varying thicknesses of 100 mm, 150 mm and 200 mm have been prepared. Thermal images of each slab sample have been captured during the heating and cooling hours of the day. To better understand the thermal profile of the slabs during the heating and cooling hours, type T- thermocouples have been inserted at different locations and the temperature profiles have been correlated with the infrared images. Effect of depth, size and type of defects were investigated using infrared thermography. To validate the results obtained, slabs were modelled in Energy 2D simulation software.

## 1 Introduction

Structural Health Monitoring (SHM) requires periodic evaluation of the “condition” of the materials, the different elements, and the full assembly of these elements constituting the structure as a whole. The condition of the structure must remain in the domain specified in the design, although this can be altered by normal aging due to usage, by the action of the environment, and by the accidental events (Balageas 2010). The diagnosis of the structure as a whole can be achieved by Non-Destructive Testing Techniques (NDTs).

A variety of different NDTs have been developed for damage detection. Ultrasonic inspection, GPR and eddy current technique are good examples of mature, well-established technologies that are widely used for crack detection. (Tadeusz Uhl 2013). These techniques are often limited to single-point measurements and require scanning when large areas need to be monitored. Also, these techniques require a physical contact to the element for evaluation making them laborious, time consuming and capital intensive. In recent years, there has been an emergence of a range of new damage detection techniques such as infrared thermography, vibration based techniques, and sensing technologies. These methods allow for global monitoring of large structures and fall into the area of SHM (Tadeusz Uhl 2013).

In theory, by directly measuring radiant infrared emission from the surface of a concrete member, thermography detects differences in surface temperature that indicate the location of thermal anomalies (Roddis 1987). These surface temperature variations result from the thermodynamic interaction of the concrete with the surrounding environment. Solar loading provides a significant driving force to create thermal gradients in the surface of concrete structures. Radiant heating from the sun elevates the temperature at the surface of the concrete, and heat is conducted through the concrete according to typical thermal diffusion principles (Priestley 1987). This thermal diffusion is disrupted by the presence of delaminations in the concrete. Heat also flows in and out of the structure by means of conduction and convection. The effects of convection occur when the ambient temperature of the air transfers heat to concrete.

ASTM D4788 2013 standardizes this method for detecting delaminations in bridge decks. According to the standard, for the delaminations to be identified by an imaging infrared scanner, there must be a temperature difference, between the delaminated or debonded area and the adjacent solid concrete of at least 0.5ºC and weather condition must include sunshine. The same have been confirmed with other research work on infrared thermography (Clark, McCann and Forde 2003) (Washer, et al. 2009). The previous literature does not include the information on the thickness of the bridge deck or the size of the delaminations. The proposed research work evaluates the variation in surface temperature when the delaminations are at different depths.

Infrared thermography is capable of detecting concrete defects as small as 50 mm in width (Bhalla, Tuli and Arora 2011). To verify this capability, specimens of size 100 x 100 x 500 mm were first heated up using four 1 kW halogen lamps for about 30 min. Defects in the form of 90 x 50 x 0.5 mm thick glossy printer paper sheets were detected using the thermal images. Conclusive remarks by Bhalla et al. are referred to the size of the defect and not the depth at which it can be detected using infrared thermography.

Similar work has been done by Yehia et al. 2007. In their work, three slabs with induced defects at different depths were cast. To mimic the real bridge deck situation three main types of defects were simulated: cracks, delamination and voids. Defects were detected using infrared thermography. However, the research work did not show the effect of the artificial defects on the surface temperature when detected using infrared thermography. Present research uses modified simulation of these defects.

There exists a need for the research in the field of infrared thermography to be able to evaluate the variation in the surface temperature due to the delamination present beneath. Present research uses the advanced FLIR E60 infrared camera and thermocouple sensors to determine the correlation.

Infrared thermography has many more advantages such as (a) ability to scan larger areas in little time, (b) ability to detect delaminations, cracks, voids, debonding between layers, and (c) low operating cost and minimal disruption to traffic and requires minimal lane closure, compared to other techniques (Yehia, Abudayyeh, et al., 2007)

## 2 Experimental work

Experimental work consisted of preparation of the specimens and inspection and validation using infrared thermography.

### 2.1 Specimen preparation

In order to evaluate the ability of infrared thermography in detecting artificial defects, a total of nine 1.8 m × 0.46 m slabs with varying thicknesses of 100 mm, 150 mm and 200 mm were prepared with four type of defects. These thicknesses were chosen to represent typical slab depths used in the field. Embedded artificial defects are shown in Figures 1 and 2. Bottom clear cover was kept at 12.5 mm so as to accelerate corrosion induced at later stages. Clear cover on sides was kept as 40 mm.

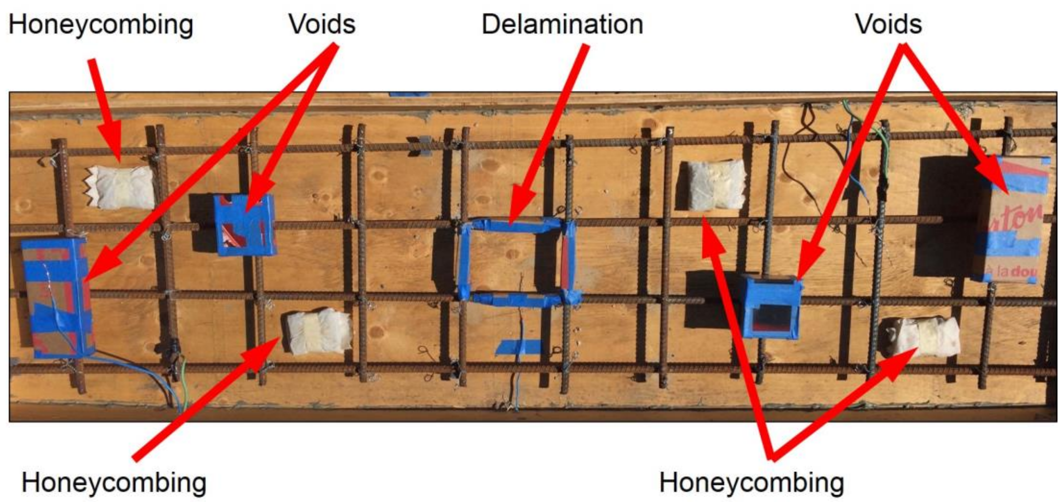


Figure 1 : Photograph showing embedded artificial defects

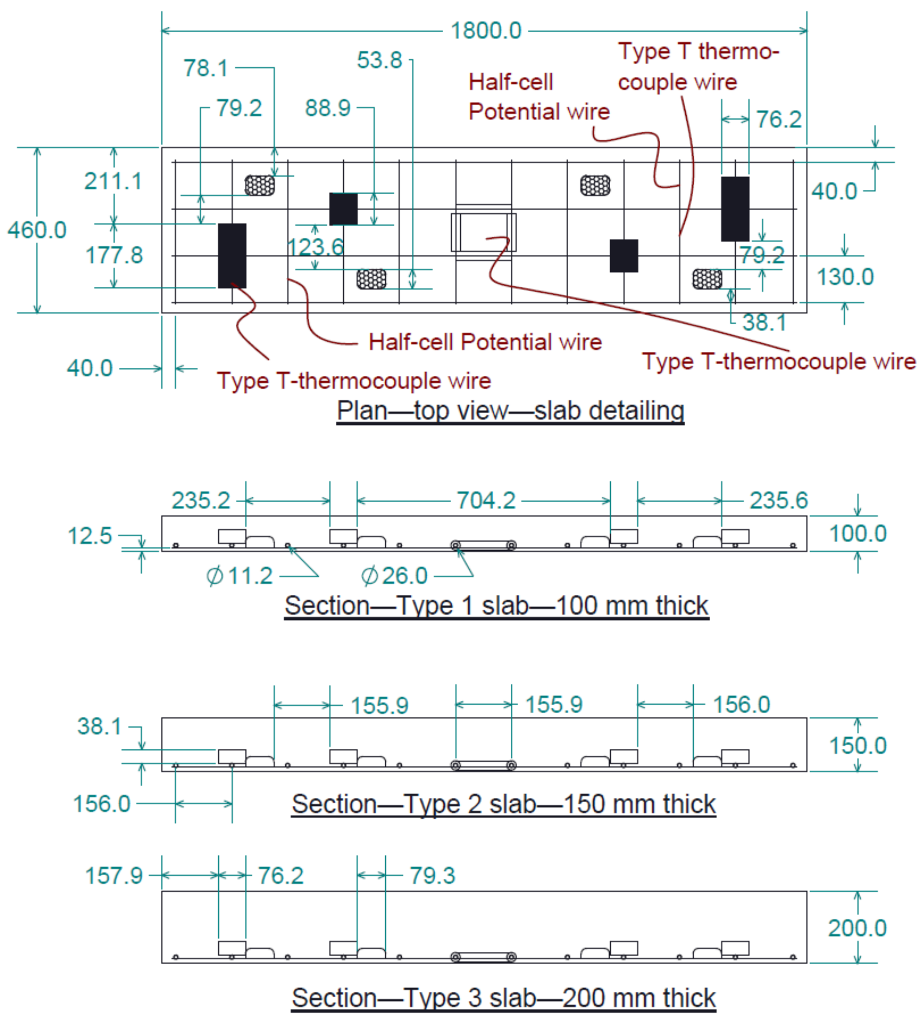


Figure 2 Cross-section of defects with dimensions (in mm)

Further details on the defects are given in the Table 1: Type of defects.

Table 1 Types of defects

| Type of Defect | Dimension (mm×mm×mm) | Location in 100 mm, 150 mm and 200 mm slab |
|---|---|---|
| Void (created using cardboard paper box) | 178×76×38, 87×76×38 | 30 mm, 80 mm,130 mm (from top) |
| Honey combing (Pocket of loose aggregates) | 50×50×20 | 80 mm, 130 mm, 180 mm (from top) |
| Delamination (Sand sleeves around rebars) | Cylindrical sleeve of dia. 20 mm | 80 mm, 130 mm, 180 mm (from top) |
| Salt | 3.4 % of the volume of the concrete | Middle third portion of the slab |

FLIR E60 (60 Hz)-Infrared Camera having a resolution of 320 × 240 pixels and a thermal sensitivity of 0.05 °C was used to detect the defects in the slabs. Images were taken during both heating and cooling times of the day. Ambient temperature was observed to be in the range of 7 to 10 °C. Three separate images covering entire top surface area of the slab were captured and are shown together in the following section.

## 2.2 Modelling and Simulation

All the slabs were modelled in Energy 2D open source software as shown Figure 3 to understand the heat transfer phenomenon occurring in the slab with voids present. Physical and thermal properties of the materials modelled are presented in the Table 2: Material Properties.

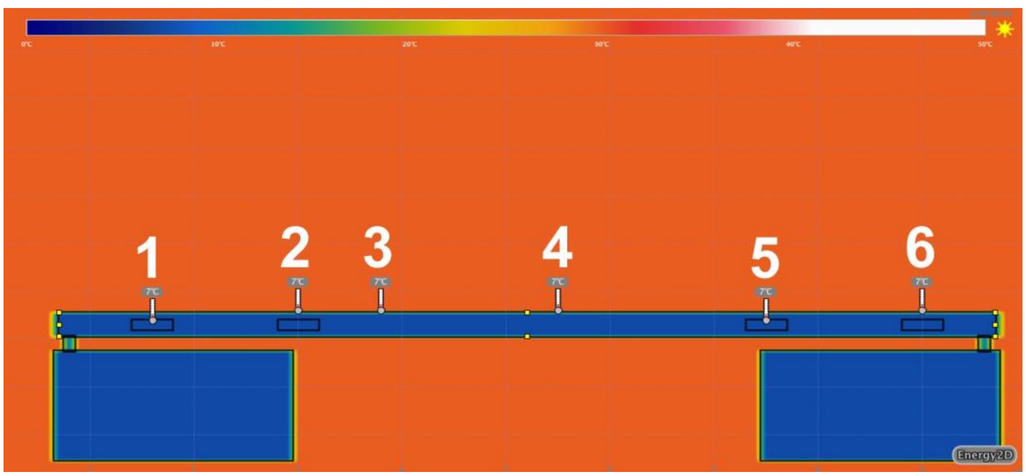


Figure 3 : Modelling and Simulation of heat transfer in Energy 2D simulation software

Table 2 Material Properties

| Material | Property | Value |
|---|---|---|
| Concrete | Initial Temperature (°C) | 7 |
| | Thermal Conductivity (W/m°C) | 1 |
| | Specific Heat (J/kg°C) | 880 |
| | Density (kg/m$^3$) | 2200 |
| | Emissivity | 0.92 |
| Air | Initial Temperature (°C) | 7 |

| | | |
|---|---|---|
| | Thermal Conductivity (W/m°C) | 0.025 |
| | Specific Heat (J/kg°C) | 1012 |
| | Density (kg/m$^3$) | 1.204 |

A total of six temperature sensors shown in Figure 3 were used to determine the temperature difference between the voids and the surrounding concrete surface temperature when an ambient temperature of 30 °C was kept. The effect of depth of void and a correlation between subsurface temperature to the surface temperature are shown in the following section.

## 3 Results and Discussions

### 3.1 Reinforced Concrete Slabs

Infrared Thermography was applied on the reinforced concrete slabs constructed at University of Victoria's Materials Lab Facility and total of three images were captured for each slab from the top. Figure 4 shows the infrared thermograph taken during the heating hours (conduction and convection) of the day. It can be seen that only the voids are detected and the temperature of the voids are hotter compared to the surrounding concrete. This was also confirmed using the thermocouple sensors inserted into the voids during casting. Figure 8 shows that there was about 1°C of temperature difference between the voids and the surface above those voids. Infrared thermographs captured after 3 pm on the same day are shown in Figures 5-7. It should be noted that even though the temperature difference between the voids and the surface above were almost same, the defects were not detected at 3 pm using infrared thermography as the ambient temperature had started falling and affected the results of infrared thermographs.

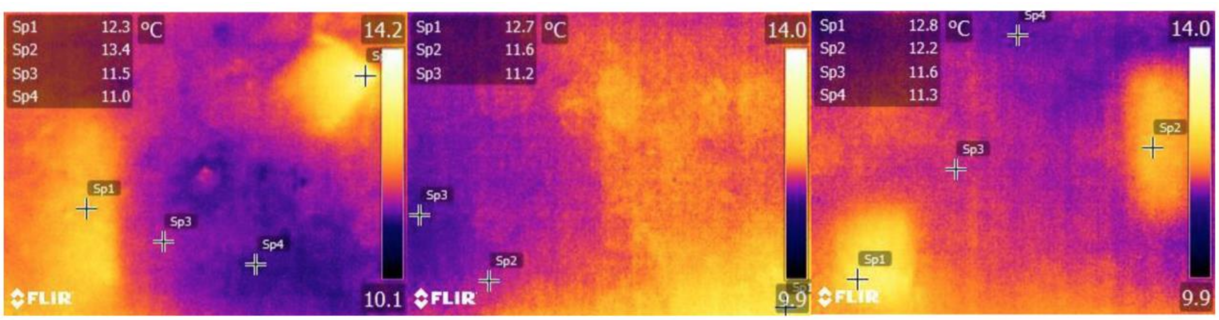


Figure 4 : Infrared Thermograph of 100 mm slab (Time: 1 pm, November 25th, 2016)

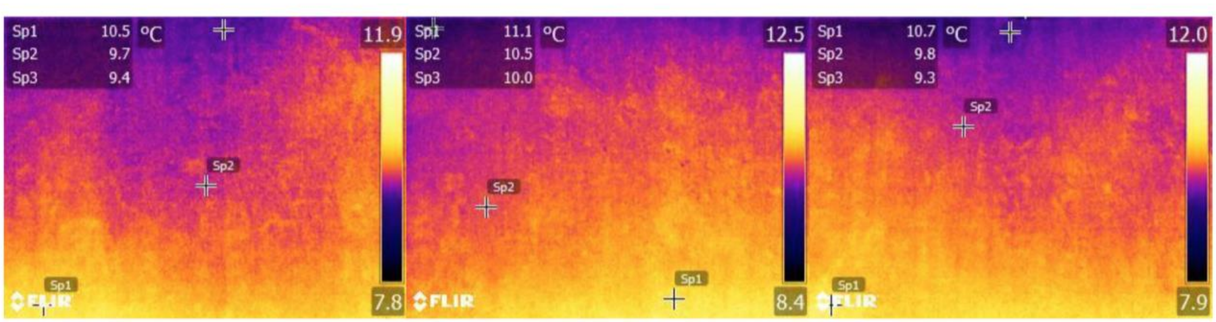


Figure 5 : Infrared Thermograph of 100 mm slab (Time: 3 pm, November 25th, 2016)

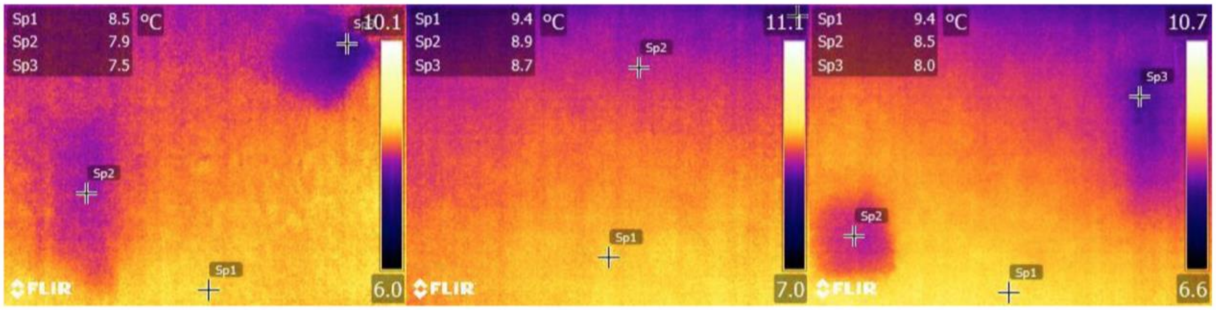


Figure 6 : Infrared Thermograph of 100 mm slab (Time: 4 pm, November 25th, 2016)

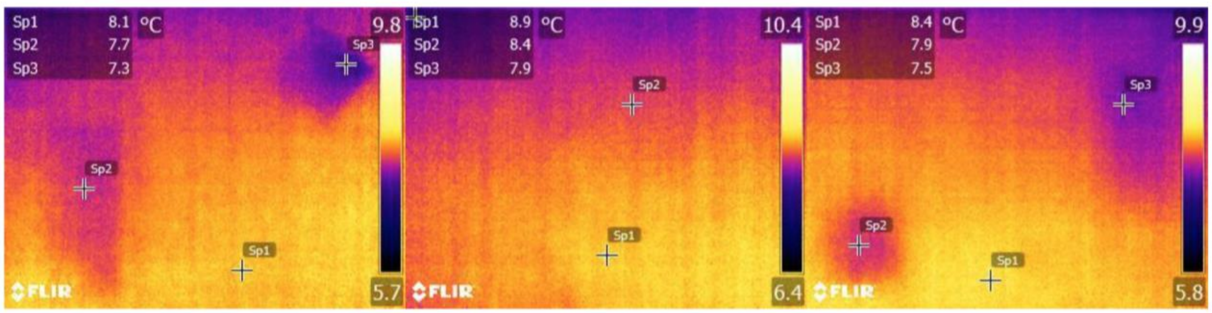


Figure 7 : Infrared Thermograph of 100 mm slab (Time: 5 pm, November 25th, 2016)

During the cooling hours (conduction and convection) after 4 pm, the voids showed lower temperature compared to the surrounding concrete. This was confirmed from the infrared thermographs (Figure 6 and 7) and the thermocouple data presented in the Figures 8 and 9. Figure 9 shows the correlation between subsurface temperature to the surface temperature.

Honeycombing and delamination were detected when infrared images were captured from the bottom surface.

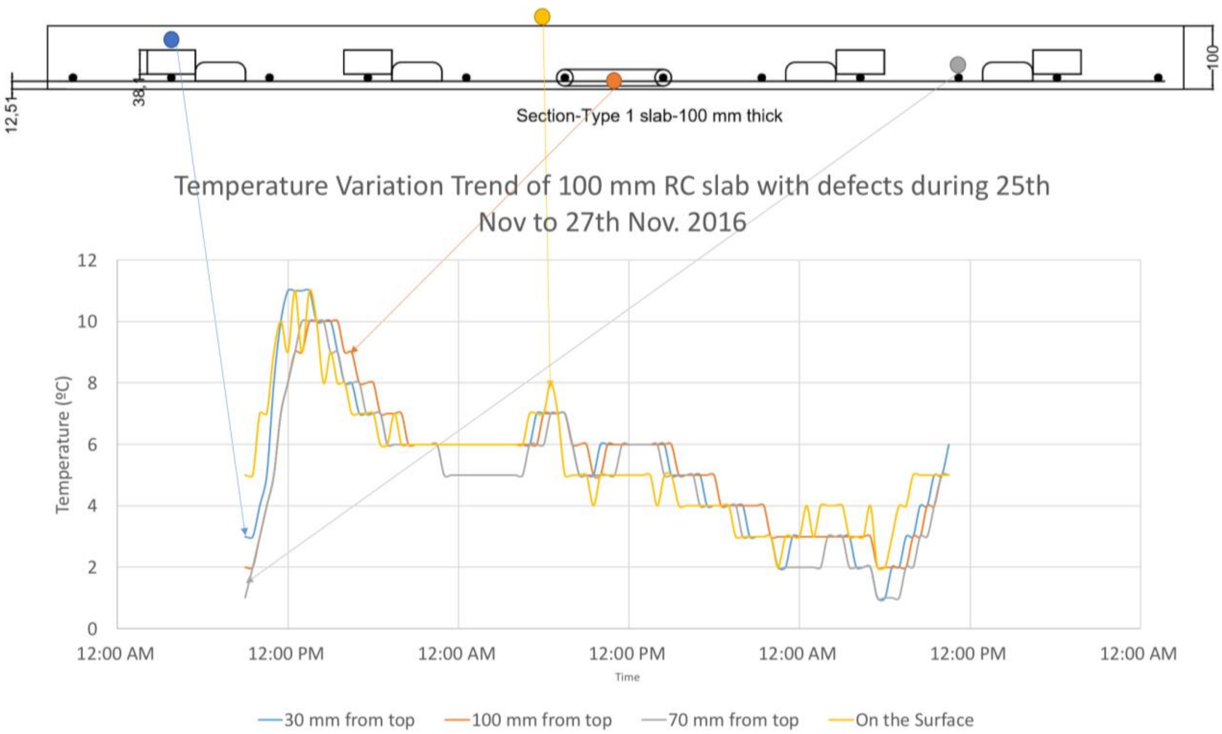


Figure 8 : Temperature variation trend of 100 mm slab using thermocouples embedded at different locations

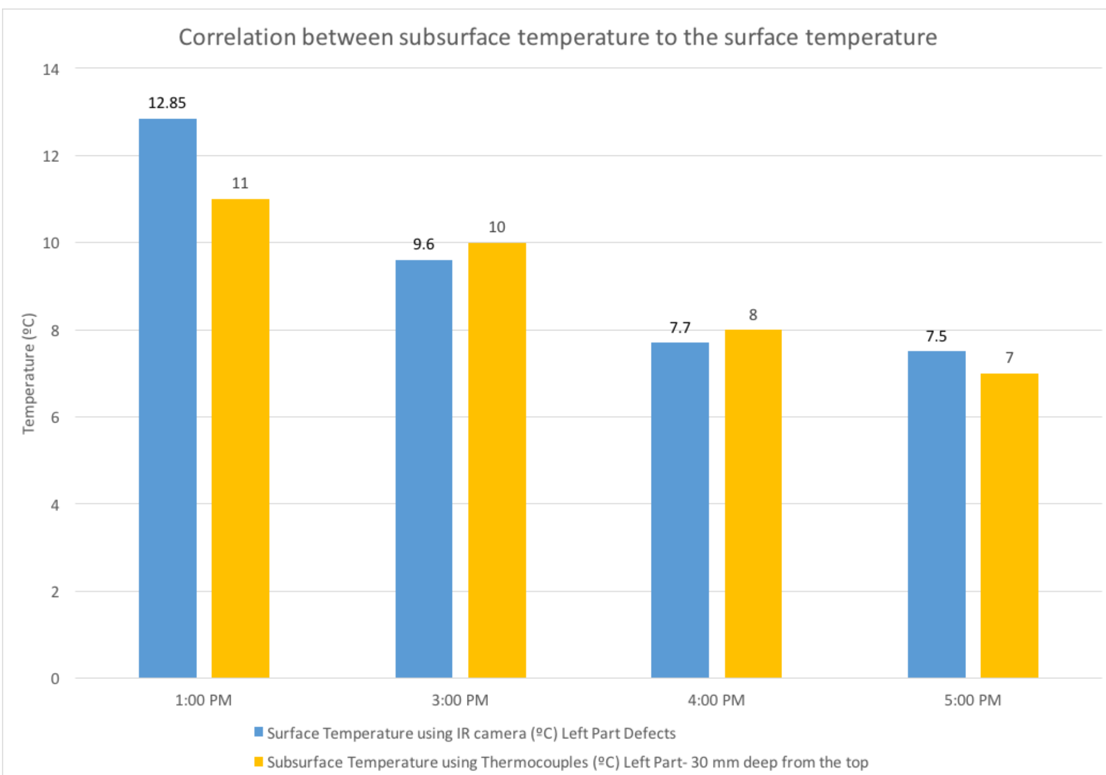


Figure 9 : Correlation between subsurface temperature to the surface temperature

Due to low ambient temperature 7-15 °C during November-December at Victoria BC, Infrared Thermography was unable to detect voids in 150 mm and 200 mm slabs. Future work involves detecting defects using infrared thermography in 150 and 200 mm slabs when the temperature scale is higher, preferably in the summer.

### 3.2 Energy 2D Simulation results

Infrared thermography failed to detect voids present in 150 and 200 mm slabs due to lower thermal gradient between voids and the surrounding sound concrete. To validate this, a simulation in Energy 2D software was run for 15 seconds and results are shown in Figure 10. It can be seen that with the same ambient conditions, as the depth of the voids increases, the surface temperature above decreases, resulting in lower temperature gradient. As the simulation was performed using different boundary conditions and with the 2-D slabs, temperature data doesn't exactly match with the experimental data. However, the temperature variation trend remains the same. Temperature gradient between voids (Left part) and the surface above for 100 mm, 150 mm and 200 mm were found to be 0.8 °C, 0.4 °C and 0.1 °C respectively.

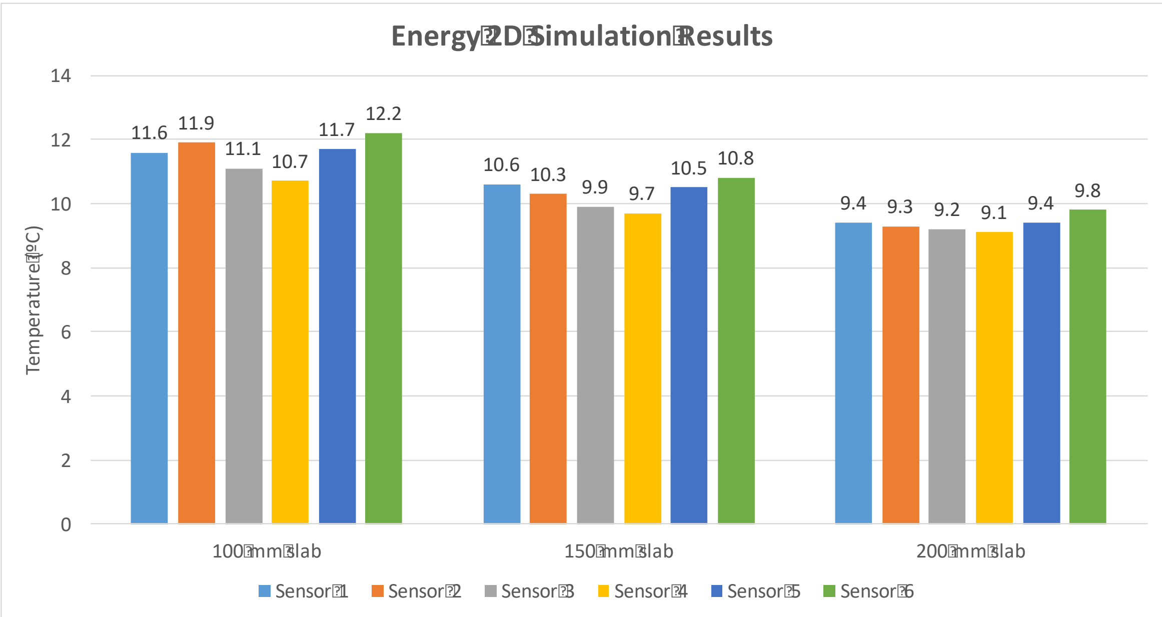


Figure 10 : Energy 2D Simulation Results

## 4 Conclusions

Results presented here show that the infrared thermography technique could be used to identify voids in concrete slabs provided there is enough temperature gradient. The technique is highly dependent on the solar loading that is being applied to produce enough temperature difference between defects and the surrounding sound concrete. Defects can not be identified if there is not enough temperature difference present between the surface above the defect and the adjacent sound concrete. Subsurface temperature data collected using thermocouple sensors strongly agrees with this. Energy 2D simulation results show that as the depth of voids increases, the temperature of the surface above decreases results into lower temperature gradient. It was found that even though the size of the void present is significant, it can not be detected if at higher depth. It requires significant solar loading to generate enough temperature gradient to be able to be detected by an infrared camera. Also, when the area of voids detected by infrared thermography compared with the actual area, the difference was found to be less than 15%.

**Acknowledgements**

Project funding received by IC-IMPACTS (India-Canada Centre of Excellence) and DST (Department of Science and Technology) is greatly appreciated.

**References**

2013. "ASTM D4788: Standard Test Method for Detecting Delaminations in Bridge Decks Using Infrared Thermography." ASTM International.

Balageas, Daniel. 2010. "Introduction to Structural Health Monitoring." In *Structural Health Monitoring*, 13-43. Wiley.

Bhalla, S., S. Tuli, and R. Arora. 2011. "DEFECT DETECTION IN CONCRETE STRUCTURES USING THERMAL IMAGING TECHNIQUES." *Experimental Techniques* 39-43.

Clark, M., D. McCann, and M. Forde. 2003. "Application of infrared thermography to the non-destructive testing of concrete and masonry bridges." *NDT&E International* 36: 265-275.

Priestley, M.J.N. 1987. "The Thermal Response of Concrete Bridges." *Concrete Bridge Engineering Performance and Advances* 143–188.

Roddis, W. 1987. *Concrete Bridge Deck Assessment Using Thermography and Radar. MS thesis.* Massachusetts Institute of Technology, Cambridge, 1987., Cambridge: Massachusetts Institute of Technology.

Tadeusz Uhl, Tadeusz Stepinski and Wieslaw Staszewski. 2013. "Introduction." In *Advanced Structural Damage Detection: From Theory to Engineering Aplications*, 1-15. John Wiley & Sons, Ltd.

Washer, Glenn, Richard Fenwick, Naveen Bolleni, and Jennifer Harper. 2009. "Effects of Environmental Variables on Infrared Imaging of Subsurface Features of Concrete Bridges." *Journal of the Transportation Research Board* 107-114.

Yehia, Sherif, Osama Abudayyeh, Saleh Nabulsi, and Ikhlas Abdelqader. 2007. "Detection of Common Defects in concrete Bridge Decks Using Nondestructive Evaluation Techniques." *Journal of Bridge Engineering* 12 (2): 215-225.